

Sediment Transport Patterns at the Essex River Inlet Ebb-Tidal Delta, Massachusetts, U.S.A.

J. Bailey Smith[†] and Duncan M. FitzGerald

Boston University
Department of Geology
Boston, MA 02215, U.S.A.



ABSTRACT

SMITH, J.B. and FITZGERALD, D.M., 1994. Sediment transport patterns at the Essex River Inlet ebb-tidal delta, Massachusetts, U.S.A. *Journal of Coastal Research*, 10(3), 752-774. Fort Lauderdale (Florida), ISSN 0749-0208.

Essex River Inlet is located along the Northern Massachusetts barrier chain between Castle Neck to the north and Coffins Beach to the south. The position of the inlet as well as the geometry of the backbarrier system are controlled by a pre-existing drainage system which, in turn, is strongly influenced by the bedrock topography. The inlet is fronted by a well developed ebb-tidal delta. The hydraulics, sediment transport patterns and morphological changes of the ebb-tidal delta have been investigated through the documentation and analysis of tidal- and wave-generated currents, grain size distributions, bedform migrational trends, swash bar development, and historical shoreline changes.

The inlet throat is increasingly dominated by ebb-tidal currents and seaward sediment transport as tidal range increases from mean towards spring tides. A similar trend exists in the marginal flood channels with increasingly stronger flood than ebb-tidal currents with increasing tidal range. These flow asymmetries explain the seaward- and inlet-oriented bedforms (sandwaves and megaripples) that floor these channels, respectively. The swash platform is dominated by landward currents and the onshore migration and coalescence of swash bars. The period of time between swash bar formation in the terminal lobe region and their eventual attachment to the landward beaches is approximately 5 to 7 years.

The channels and swash platform are parts of clockwise (updrift half of ebb-tidal delta) and counter-clockwise (downdrift half of ebb-tidal delta) sediment gyres that circulate sand within the ebb-tidal delta and account for the sand that bypasses the inlet. Sediment transport rates determined using a variety of means (*i.e.* MADDOCK's (1969) equation, swash bar migration data, morphological changes) indicate that the main ebb channel can easily remove the sand supplied from the marginal flood channels and across the channel margin linear bars. Moreover, calculated sand transport rates in the main ebb channel infer an order-of-magnitude, more sand is moved across the swash platform than is indicated by the migration of the swash bars. This suggests that far more sand is circulated within the sediment gyres than bypasses the inlet.

ADDITIONAL INDEX WORDS: *Tidal inlet, ebb-tidal delta, sediment transport patterns, morphologic changes, sand circulation gyre, onshore bar migration.*

INTRODUCTION

Ebb-tidal deltas are accumulations of sand which front tidal inlets and are formed by the interaction of tidal- and wave-generated currents. Numerous authors (HAYES, 1975, 1979; HINE, 1975; OERTEL, 1975; HUBBARD, 1977; FINLEY, 1978; FITZGERALD and NUMMEDAL, 1983; FITZGERALD, 1984; SHA, 1990) have documented the physical processes and resulting sediment circulation patterns which exist at ebb-tidal deltas. Essex River Inlet, the subject of our research, was used by HAYES (1975) to develop one of the first morphologic and hydrodynamic models of ebb-tidal deltas. Other investigations of the Essex estuarine system include a bedform study by BOOTHROYD

and HUBBARD (1974), and a stratigraphic study by SOM (1990).

With an average significant wave height of 1.00 m and mean tidal range of 2.60 m, Essex River Inlet plots in HAYES' (1979), and NUMMEDAL and FISCHER's (1978) mixed-energy tide-dominated coastline settings. Generally, depositional shorelines of this type (Table 1) have relatively short barrier islands, numerous tidal inlets, and backbarriers consisting of marsh tidal creeks (*e.g.* Central South Carolina) or intertidal flats (*e.g.* East Friesian Islands). Open water areas comprise only a small percentage of the backbarrier region. Characteristically, tidal inlets along these coasts have well-developed ebb- and flood-tidal deltas, although in South Carolina and parts of Georgia flood-tidal deltas appear to be absent. There may, in fact, be flood-tidal deltas in these regions, but they are probably covered by salt marshes and simply have not been identified.

93080 received 8 August 1993; accepted in revision 22 November 1993.

[†] Present address: U.S. Army Engineer Waterways Experiment Station, Coastal Engineering Research Center, 3909 Halls Ferry Road, Vicksburg, MS 39180-6199, U.S.A.

Table 1. Mixed-energy tide-dominated system parameters. Unless otherwise noted by footnotes, referenced data include: tidal data taken from U.S. DEPARTMENT OF COMMERCE (1994); average significant wave height data borrowed from JENSEN (1983); ebb-tidal delta and flood-tidal delta parameters borrowed from several U.S. DEPARTMENT OF COMMERCE Nautical Charts; and tidal prism borrowed from JARRETT (1976). Offshore extent of ebb-tidal delta and distance to the 7 m contour measured from the inlet throat.

Region	Ebb-Tidal Delta (average values)							Flood-Tidal Delta Degree of Development/ Exposure of Bars
	Mean (Spring) Tidal Range (m)	Average Signif. Wave Height (m)	Degree of Development/ Exposure of Bars	Offshore Extent of Ebb-Tidal Delta (m) ¹	Regional Offshore Slope (to 7 m contour)	Inlet Throat Width (m) (MLW)	Spring Tidal Prism (m ³ /tidal cycle)	
Northern Massachusetts Coast (Merrimack Embayment) ²	2.60 (3.10)	1.00	Well-developed, Sub/ Intertidal	1,500	0.0065	320	2.3×10^7	Well-developed, Intertidal to Subtidal
Southern New Jersey Coast	1.20 (1.40)	0.60	Well-developed, Sub/ Intertidal	2,500	0.0042	830	5.1×10^7	Well-developed, Subtidal to Intertidal
Virginia Coast	1.10 (1.40)	0.65	Well-developed Sub/ Intertidal	4,900	0.0029	840	6.0×10^7	Well-developed, Subtidal to Intertidal
Central South Carolina Coast ⁴	1.60 (1.90)	0.70	Well-developed, Intertidal	1,700	0.0028	350	1.6×10^7 ⁵	Lacking to poorly-devel- oped, Subtidal to Inter- tidal
Southern South Carolina Coast ^{4b}	1.90 (2.40)	0.60	Well-developed, Intertidal	4,800	0.0015	730	1.1×10^8	Lacking to poorly-devel- oped, Subtidal to Inter- tidal
Georgia Coast ¹	2.20 (2.70)	0.90	Well-developed, Intertidal	8,000	0.0010	2,500	1.7×10^8	Lacking to poorly-devel- oped, Subtidal to Inter- tidal
Gulf of Alaska Coast (Copper River Delta Barrier Islands) ⁷	2.80 (3.40)	1.50	Well-developed, Subtidal	2,300	0.0018	2,500	8.6×10^8 ^{8b}	Well-developed, Subtidal to Intertidal
German East Friesian Island Coast ⁹	2.55 (2.75)	1.55	Well-developed, Sub/ Intertidal	5,200	0.0024	2,700	2.9×10^8	Well-developed, Intertidal
Netherlands West Friesian Island Coast ⁹	1.90 (2.40)	1.15	Well-developed, Sub/ Intertidal	5,100	0.0034	4,000	3.5×10^8	Well-developed, Intertidal

¹Distance to terminal lobe

²Data from SOM (1990) and SMITH (1991)

³Data from NUMMEDAL *et al.* (1977)

⁴Includes Price, Capers, Dewees, Breach, and Lighthouse Inlets

⁵Data from FITZGERALD and FITZGERALD (1977)

⁶Includes Stono, North Edisto and Fripp Inlets

⁷Data from HAYES (1976, 1979)

⁸Spring tidal prism for the Copper River Delta Barriers based on JARRETT's (1976) relationship for Strawberry and Egg Island Channels, and the channel to the east of Kokinhenik bar

⁹Data from POSTMA (1982), FITZGERALD, PENLAND and NUMMEDAL (1984), and SHA (1989, 1990)

Although mixed-energy, tide-dominated inlets have been investigated throughout the world, few of these studies have been in regions with upper mesotidal ranges (Spring TR > 3.0 m) and have focused on the ebb-tidal delta. Of the inlet coasts listed in Table 1, only the Northern Massachusetts, and the Gulf of Alaska have spring tidal ranges greater than 3.0 m. Northern Massachusetts inlet systems are considerably smaller than those of the Gulf of Alaska, both in size of the ebb-tidal delta, and width of the inlet throat (Table 1). These differences are explained, in part, by the smaller tidal prisms of Northern Massachusetts Inlets. Essex River Inlet and other Northern Massachusetts inlets are close in size to those of Central South Carolina despite a tidal range which is almost twice as large in Northern Massachusetts. The purpose of this research has been to document the hydraulic and sediment transport patterns at Essex River Inlet, particularly those in the ebb-tidal delta system, and to compare these findings with other ebb-tidal deltas of similar size or tidal range.

PHYSICAL SETTING

Essex River Inlet is one of several tidal inlets located along the 35-km barrier island chain of the Merrimack Embayment in northeastern Massachusetts (Figure 1). The inlet is bordered by two late Holocene barrier islands, Crane Beach to the northwest and Coffins Beach to the southeast. The barrier islands of this mixed-energy tide-dominated setting are relatively short and are separated by tidal inlets with well developed ebb- and slightly smaller flood-tidal deltas (HAYES, 1979). The backbarrier consists of marshes incised by tidal creeks which enlarge to small bays near the inlet openings.

The tides at Essex River Inlet are semidiurnal and have a mean tidal range of 2.60 m and a mean tidal prism of $2.01 \times 10^7 \text{ m}^3$. During spring tides, these parameters increase to 3.10 m and $3.04 \times 10^7 \text{ m}^3$, respectively. The maximum diurnal inequality during spring tides is 0.60 m.

A 20-year hindcast study indicates that the predominant wave energy is from the east-northeast (JENSEN, 1983; Station 21). The annual frequency distribution of wave heights and wave periods associated with this study shows that 60% of the wave heights are between 0.00 and 0.99 m, and 41% of the wave periods are between 3.0 and 4.9 seconds. The average significant wave height is

1.0 m and the maximum significant wave height is 8.7 m.

The dominant east-northeast wave climate in the Merrimack Embayment produces a southerly longshore movement of sand which is evidenced by: 1) the growth of recurved spits on the southern downdrift ends of Crane Beach and Plum Island; 2) a southerly decrease in grain-size fining trend within the Merrimack Embayment (SHALK, 1936; GOODBRED and MONTELLO, 1989) and; 3) a southerly decrease in offshore slope suggesting that Cape Ann headland is acting as a terminal groin (Figure 1). Using the wave energy flux method (U.S. ARMY CORPS OF ENGINEERS, 1984), the longshore sediment transport is estimated to be 125,000 m^3/year along Plum Island and 34,000 m^3/year along Crane Beach. The reduced sediment transport rate for Crane Beach is due to the flatter offshore slope, a change in the shoreline trend, and a smaller breaker angle during dominant storm wave energy conditions.

Inlet and ebb-tidal delta terminology used in this paper follows that of HAYES (1979) (Figure 2A).

BARRIER ISLAND AND TIDAL INLET DEVELOPMENT

The sediment supply for the formation of this barrier island system is believed to come primarily from the reworking and onshore transport of sand comprising the lowstand Merrimack River Delta in the form of a landward migrating sand sheet and transgressive barrier islands during the late Holocene (circa 8,500 to 4,000 years BP) (EDWARDS, 1988; FITZGERALD, 1993). Additional sediment was introduced to the system through the erosion of the drumlins and other glacial sediments that were intercepted during the transgression (*cf.* BOYD *et al.*, 1987). The stabilization of transgressive barrier islands to bedrock highs, drumlins, and other pinning points occurred as the rate of sea level rise decreased (circa 3,000 to 4,000 years BP) (EDWARDS, 1988; FITZGERALD, 1993). The stabilization of the barrier island system during the late Holocene Epoch is probably attributed, in part, to an increase in sediment supply that was coincident with slowing sea level rise (*cf.* HINE *et al.*, 1979; BOYD *et al.*, 1987). The position of inlets along the barrier island chain is likely related to the presence of former river valleys (Merrimack, Parker, Ipswich and Essex Rivers), drumlins, and bedrock outcrops (FITZGERALD, 1993).

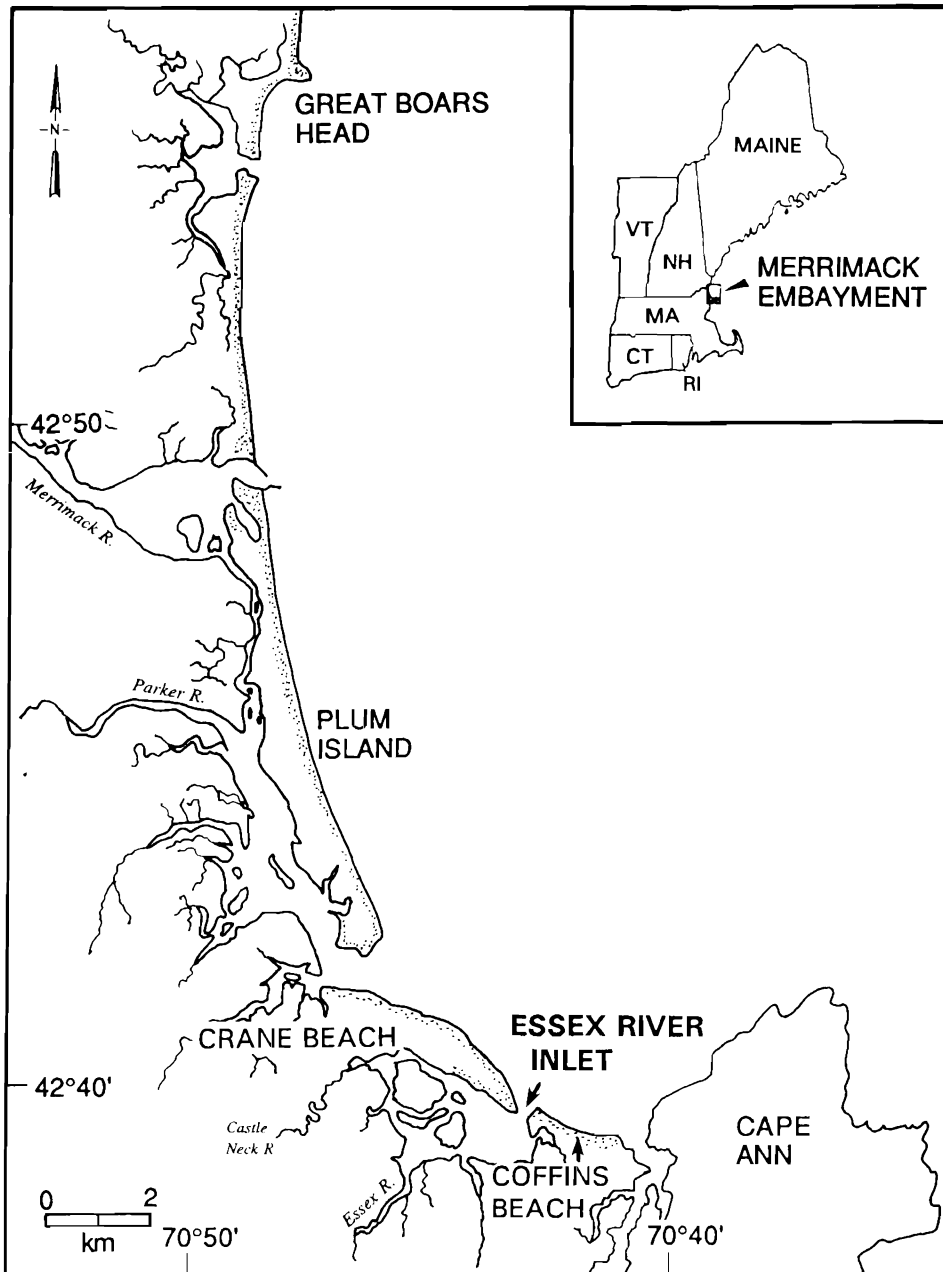


Figure 1. Location of Essex River Inlet with respect to other inlets in the Merrimack Embayment.

Radiocarbon dates from shells in offshore sediment cores (OLDALE, 1985) and basal salt water and fresh water peats (MCINTYRE and MORGAN, 1964; MCCORMICK, 1968; NEWMAN *et al.*, 1980)

suggest that Plum Island began forming sometime after 6,300 years BP. It is possible that Crane Beach and Coffins Beach are somewhat younger but of similar age.

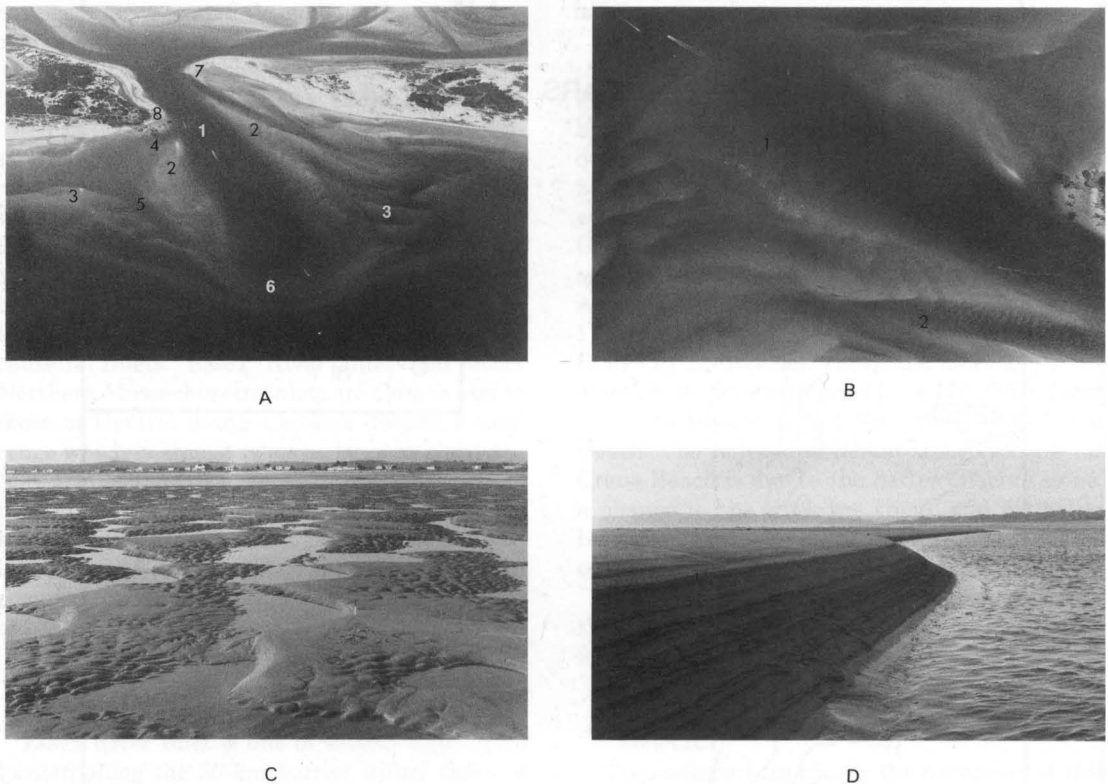


Figure 2. Photographs of Essex River ebb-tidal delta. (A) Oblique aerial view to landward with Crane Beach to the right and Coffins Beach to the left. The numbered sedimentary environments are: (1) main ebb channel; (2) channel margin linear bar; (3) swash bar/platform; (4) marginal flood channel; (5) swash platform channel; (6) terminal lobe; and (7) Crane Beach spit platform. Feature (8) is Twopenny Loaf Bedrock headland. (B) Oblique aerial photograph showing: (1) main ebb channel ebb-oriented sandwaves and; (2) updrift marginal flood channel flood-oriented sandwaves. Photographs A and B taken 27 May 1989. (C) Groundview of ebb-oriented cusped megaripples located at seaward portions of the downdrift channel margin linear bar showing the lateral branching of the main ebb channel across the downdrift channel margin linear bar. Average bedform wavelength and height is 2.8 m and 0.2 m, respectively. (D) Groundview of swash bar slipface showing landward migration of the downdrift swash bar. The height of the slipface is approximately 1.0 m. Photographs C and D taken at low tide on 26 May 1990.

METHODS

Morphologic changes and sand circulation patterns at the inlet were determined from field data collected between Spring 1989 and Fall 1990, and from historical information. Tidal- and wave-generated currents were recorded using a Marsh-McBirney electromagnetic current meter during seven tidal cycles (tidal range of 1.8 to 3.0 m) at 17 locations on the ebb-tidal delta and in the inlet channel. Measurements were taken at three depths through the water column and each station was occupied at least once an hour during the hydrography. Fathometer profiles in the channels provided information concerning bedform size and

orientation, and channel geometry. Intertidal bedforms were mapped on 12 occasions during the study period. Bedform nomenclature in this paper follows that of previous bedform studies of Essex River Inlet (BOOTHROYD and HUBBARD, 1974).

Documentation of the formation, onshore migration and coalescence of swash bars was performed by pace and Brunton Compass mapping of the ebb-tidal delta at low water three times during the study period. Boundaries of individual bars were defined by 0.5 to 2.0 m high slipfaces on their landward side and abrupt changes in slope along the main ebb channel. A water depth of 0.5

m (MLW) was used to define the seaward extent of the bars, the actual water depth of which was dependent upon the time of the survey and the tidal range for that particular day. Onshore migration of bars was also determined more frequently by monitoring the distance between permanent stakes and bar slipfaces. The volume of the ebb-tidal delta was calculated using a method suggested by DEAN and WALTON (1975).

Shoreline changes were determined from 13 beach surveys extending from the back dune across the marginal flood channel to the distal portion of the ebb-tidal delta. The profiles were surveyed five times during the study period. Longer-term shoreline and ebb-tidal delta morphologic changes were determined from the analysis of vertical aerial photographs dating back to 1943. Thirty-four sediment samples were collected from the beach, and 177 samples were collected from ebb-tidal delta subtidal and intertidal locations utilizing a Van Veen grab apparatus.

Wave refraction patterns in the vicinity of the inlet were investigated from oblique aerial photographs taken on 27 May 1989 near high tide conditions. During this time, wave characteristics were recorded along the adjacent beaches.

RESULTS

Channel Morphology

The Essex River Inlet throat has a maximum depth at mean sea level (MSL) of 13.7 m, a width of 320 m, and a cross-sectional area of 1,850 m² (1,350 m² at MLW) (Table 2; Figure 3, Profile A–B). The spring tidal prism of the Essex River Inlet (3.04×10^7 m³/tidal cycle) plotted against the throat cross-sectional area falls within the 95% confidence limits for inlets on the Atlantic Coast with one or no jetties (JARRETT, 1976) which suggests that the size of the inlet is in a state of stability or dynamic equilibrium.

Twopenny Loaf, a bedrock outcrop at the northern end of Coffins Beach, and other bedrock highs in the backbarrier stabilize the position of the inlet throat, flood-tidal delta, and portions of the inlet channel (Figure 2A) (SOM, 1990). The asymmetric profile of the inlet throat, deeper along the southern side, is a result of the backbarrier tidal channels draining along the southern side of the channel and the preferential delivery of sand to the northern side of the channel by the dominantly southerly longshore transport system.

From the inlet throat, the main ebb channel

Table 2. Essex River Inlet parameters (relative to MSL at the inlet throat). The spring and mean average peak velocities were determined through regression analysis of maximum current velocities measured at the Essex River Inlet throat during different tidal conditions.

Parameter	Value
Width (m)	320
Maximum depth (m)	13.7
Average depth (m)	6.8
Cross sectional area (m ²) at:	
Mean sea level	1,850.0
Mean low water	1,350.0
Hydraulic radius	4.0
Highest recorded velocity (cm/sec)	119.0
Current Velocities (cm/sec)	
Peak	110.0
Mean	93.0
Tidal prism (m ³)	
Spring	3.04×10^7
Mean	2.01×10^7
Ebb-tidal delta sediment volume (m ³)	3.53×10^6
Ebb-tidal delta distance offshore (km) (to the terminal lobe)	1.2

shoals to a depth of 3.5 m (MSL) and increases in width to 400 m at the terminal lobe (Figure 3, Profile C–H). At the confluence of the main ebb channel and the southern marginal flood channel, there is a slight deepening of the channel due to increased flow, turbulence and scour during flooding tides (Figure 3, Profile C–H).

It has been shown by WALTON and ADAMS (1976) that the volume of sand contained in the ebb-tidal delta correlates well with the mean tidal prism for inlets along coasts with similar wave energy. At Essex River Inlet, the ebb-tidal delta sediment volume (3.53×10^6 m³) and mean tidal prism (2.01×10^7 m³/tidal cycle), plot close to the regression curve determined for moderately exposed coasts (WALTON and ADAMS, 1976).

Tidal- and Wave-Generated Currents

Due to the small drainage areas of both Castle Neck and Essex Rivers, little freshwater discharge is contributed to the Essex River Inlet except during periods of spring freshets. Consequently, the water column at the inlet is well-mixed and the flow unstratified. Regression analysis of maximum and mean ebb and flood current velocities, versus tidal range measured over five tidal cycles at the inlet throat, indicate that for tidal ranges above mean tidal conditions the inlet is domi-

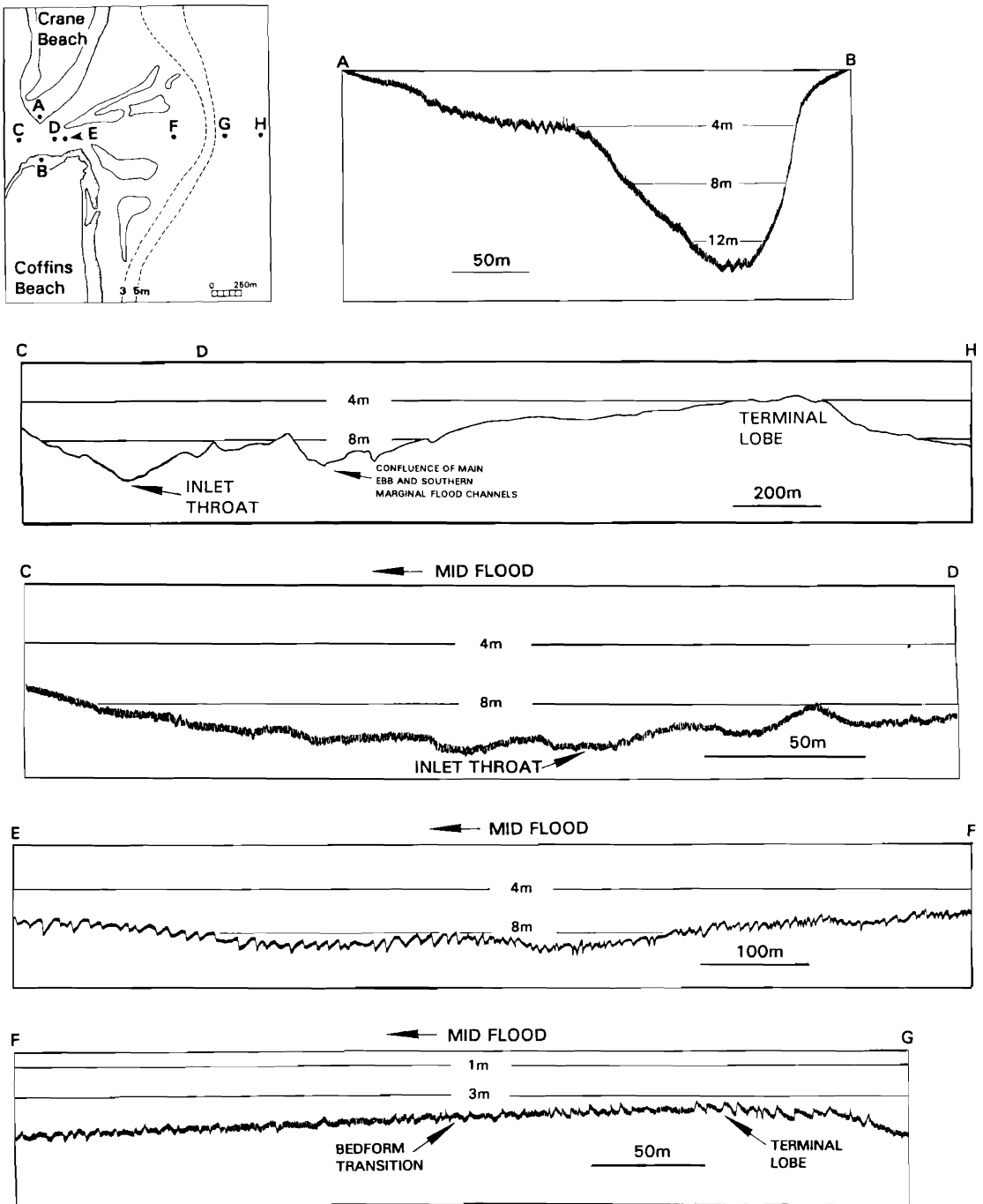


Figure 3. Bathymetric profiles of the inlet throat and main ebb channel illustrating the morphology of the channel, and bedform distributions and orientations.

nated by ebb-tidal flow (SMITH, 1991). However, it should be noted that some of the individual stations monitored during the hydrographies exhibited stronger flood currents than ebb currents. For example, as seen in Figure 4, maximum flood velocities were greater than maximum ebb velocities at Stations 2 and 3. This apparent discrepancy is explained by the fact that the flood-tidal range was 33 cm higher than the ebb-tidal range during the period when the currents were measured. Moreover, the currents in the thalweg were clearly ebb-dominated (Figure 4, Station 4; Figure 3, Profile A-B). Tidal currents are only slightly asymmetric with respect to time as maximum flood-tidal currents monitored over 5 individual tidal cycles occur 2.75 hr before high water while maximum ebb-tidal currents occur 2.75 hr after.

Time-velocity asymmetry at tidal inlets has been explained as a function of inlet efficiency and filling characteristics of the backbarrier (KEULEGAN, 1967; MOTA-OLIVEIRA, 1970; NUMMEDAL and HUMPHRIES, 1978; FITZGERALD and NUMMEDAL, 1983) and distortions of the tidal wave (BOONE and BYRNE, 1981; AUBREY and SPEER, 1985). At Essex River Inlet, average tidal durations at the throat section were 6:20 and 6:05 hr, for flood- and ebb-tidal cycles, respectively. The shorter ebb than flood duration results in stronger average ebb-tidal currents. This velocity asymmetry is emphasized in the main ebb channel due to the channel margin linear bars that constrict the ebb flow late in the ebb cycle and deflect the flood flow to the periphery of the inlet early in the flood cycle.

Currents in Main Ebb Channel

Ebb-tidal currents in the main ebb channel decrease in a seaward direction due to the increase in channel width and subsequent lateral branching of ebb-tidal currents through spillover channels at the distal portions of the channel margin linear bars (OERTEL, 1975), and gradual decrease in intertidal exposure of the channel margin linear bars. For example, on 12 June 1990 maximum ebb currents decreased from 40 cm/sec halfway out the main ebb channel (Station 5) to 30 cm/sec near the distal portion of the main ebb channel (Station 6) (Figure 4). Using regression curves of maximum ebb-tidal currents versus tidal range (see SMITH, 1991), a maximum current velocity of 83 cm/sec is predicted at the inlet throat (Station 4) using a 12 June 1990 ebb tidal range of 246 cm.

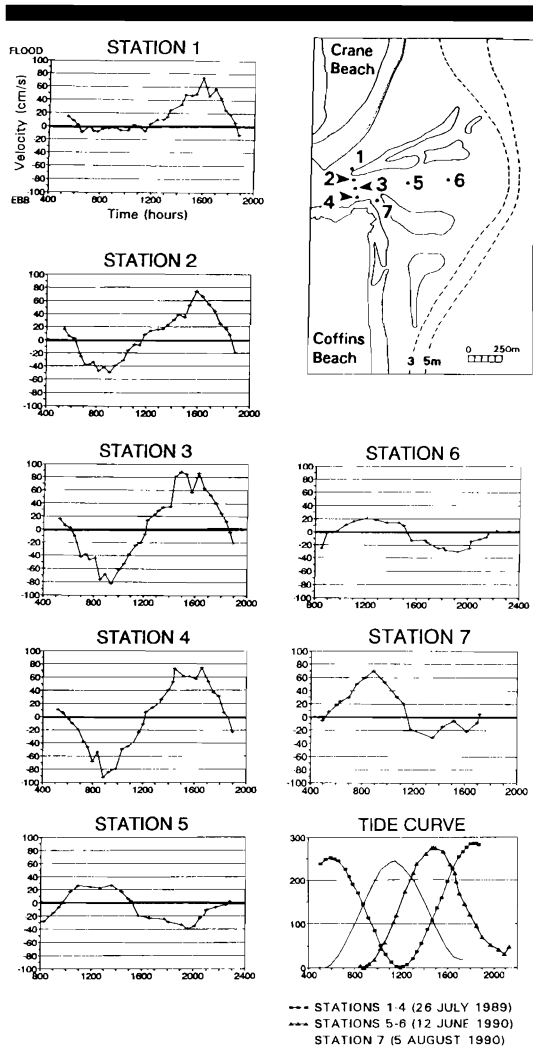


Figure 4. Tide curves and time-series of current velocities of the main ebb channel and updrift marginal flood channel. Stations 1-4 measured on 26 July 1989, Stations 5-6 measured on 12 June 1990, and Station 7 measured on 5 August 1990.

This velocity is twice as large as the velocity halfway out the main ebb channel (Station 5).

Currents in Marginal Flood Channels

Current measurements indicate that both marginal flood channels are dominated by flood currents with respect to velocity and time. The northern updrift channel, which has a cross-sectional area of 270 m² and a maximum water depth of 3.7 m at MSL, had maximum and mean flood currents which ranged from 34 to 82 cm/sec and 19

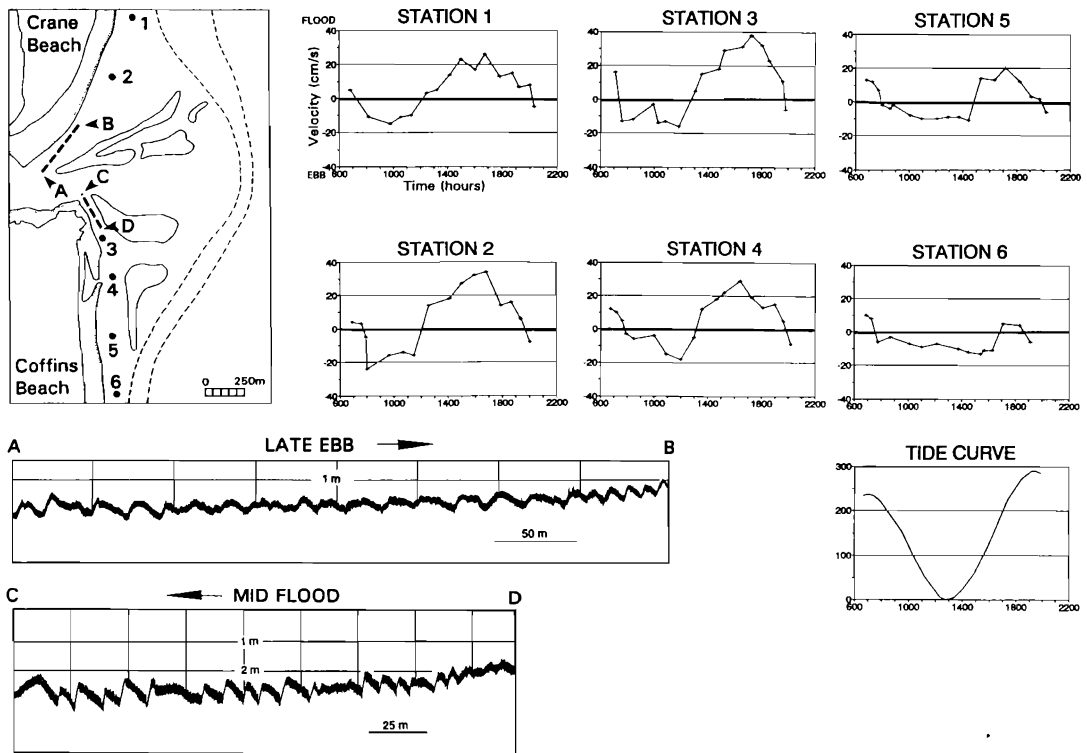


Figure 5. Tide curve and time-series of current velocities in the marginal flood channels and along the inlet beaches as recorded on 17 July 1990 (wave heights of 0.0–0.5 m from the north-northeast). Fathometer profiles of both marginal flood channels close to the main ebb channel illustrate the dominance of inlet directed sediment transport in these channels.

to 35 cm/sec, respectively, over several hydrographies. This compares to 9 to 24 cm/sec, and 5 to 15 cm/sec, for maximum and mean ebb current velocities, respectively (Figure 4, Station 1). Likewise, the downdrift marginal flood channel (cross-sectional area of 230 m² and a maximum depth of 4.2 m at MSL) exhibited stronger flood currents with maximum velocities ranging between 29 and 70 cm/sec, which compared to 15 to 32 cm/sec for maximum ebb velocities (Figure 4, Station 7). Mean flood velocities varied from 16 to 38 cm/sec while the mean ebb velocities ranged from 9 to 17 cm/sec.

Generally, the duration of flood currents in the marginal flood channels exceeded that of the ebb by 1½ to 3 hr. This fact can be related to flow segregation at the inlet (HAYES, 1977) and wave set up ponding water between the channel margin linear bar and the adjacent beach. Later in the tidal cycle, flood currents enter the inlet through

the main ebb channel and over the channel margin linear bars.

Currents along Inlet Beaches

Currents measurements along the inlet beaches indicate a strong dominance of inlet-directed flow (Figure 5) (*cf.* HUBBARD, 1975; FITZGERALD, 1976; FINLEY, 1978; SHA, 1989). Along the updrift side of the inlet, maximum flood currents reached 35 cm/sec and exceeded the ebb currents by 10–15 cm/sec (Figure 5, Stations 1 and 2). In addition, flood durations averaged over 3:30 hr longer than the ebb cycle. Along the downdrift inlet shoreline, the flood dominant currents decrease away from the inlet. Maximum flood currents at Station 3 (Figure 5) of 32 cm/sec exceeded ebb currents by 10–15 cm/sec in velocity and 1:37 hr in duration. South of Station 3, maximum flood currents of 20 cm/sec exceeded the ebb currents by 5 cm/sec and 1:50 hr in duration (Station 5). South of the con-

finer of the ebb-tidal delta, maximum ebb currents of 15 cm/sec exceeded the flood currents by 5 cm/sec and 7:38 hr (Station 6). This suggests that at Station 6 angular wave approach reestablishes the dominant southerly longshore currents of this region.

The dominance of inlet-directed flow along northern Coffins Beach was also evidenced by wave refraction patterns as documented in an aerial survey of the inlet on 27 May 1989. During this time, northeast waves with periods of 8 sec and significant wave heights of approximately 1.0 m diverged around the downdrift portion of the ebb-tidal delta. It is likely that refraction patterns are influenced by the presence and extent of swash bars on the ebb-tidal delta and change as the swash bars migrate and attach to the onshore beach (cf. FITZGERALD, 1984).

Currents on Ebb-Tidal Delta Platform

Landward flow dominates the ebb-tidal delta platform due to the combined effects of wave energy and tidal current segregation (HINE, 1975; OERTEL, 1975; FITZGERALD, 1984). Channel margin linear bars serve to confine the ebb jet which shelters much of the delta platform from ebb-tidal currents. During the initial flood stage, tidal currents move into the inlet through the marginal flood channel. At higher stages, currents flow across the delta platform as well as through the main ebb channel. In addition to the tidal flow, shoaling and breaking waves generate landward flow which enhances flood currents and retards the ebb currents. As illustrated in Figure 6, landward flow produced by the combined flood tidal- and wave-generated currents strongly dominates several environments on the delta platform including the distal swash bar (Station 1), the distal portion of the channel margin linear bar (Station 2), and the southern proximal bar complex (coalescent swash bars) (Station 4). The distal portion of the downdrift channel margin linear bar (Station 3) is less sheltered from ebb-tidal currents in the main ebb channel and therefore is only slightly flood dominant.

Sediment Characteristics

The tidal inlet and ebb-tidal delta system consist of well- to very well-sorted (0.21ϕ – 0.50ϕ) fine to medium sand (1.75ϕ – 2.50ϕ). The generally fine-grained nature of the system is a function of the overall fine-grained sediments comprising the adjacent beaches (GOODBRED and MONTELLO, 1989)

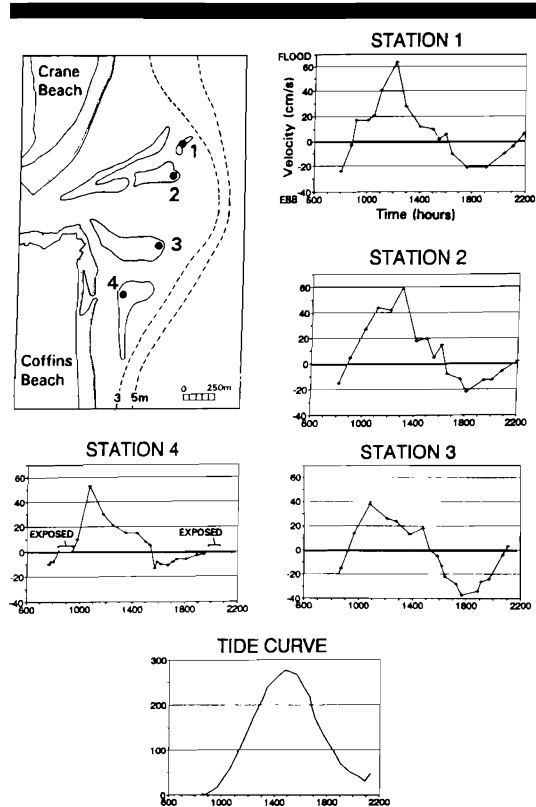


Figure 6. Tidal- and wave-induced currents recorded in the distal portion of the ebb-tidal delta on 12 June 1990 (wave heights of 1.0 m from the north-northeast). The majority of distal portions of the ebb-tidal delta are strongly flood-dominant (Stations 1, 2 and 4), excepting the distal downdrift channel margin linear bar is only slightly flood-dominant (Station 3).

and the offshore (ANAN, 1971). The grain size variations that do exist can be related to differences in tidal- and wave-energy.

Grain-size data indicate that there are slight changes in grain size among the environments excepting the main ebb channel. The first of three trends is a seaward fining of grain size from the inlet throat ($d_m = 1.70\phi$) to the seaward portion of the ebb-tidal delta ($d_m = 2.62\phi$) which presumably results from a decrease in current velocity (cf. NELLIGAN 1982; SHA, 1989). Sediments of the main ebb channel are very well- to well-sorted (0.32ϕ to 0.41ϕ).

A second and unexpected trend is the finer-grained nature of updrift portions of the ebb-tidal delta ($d_m = 2.22\phi$) and Crane Beach ($d_m = 2.16\phi$), as compared to downdrift portions of the ebb-

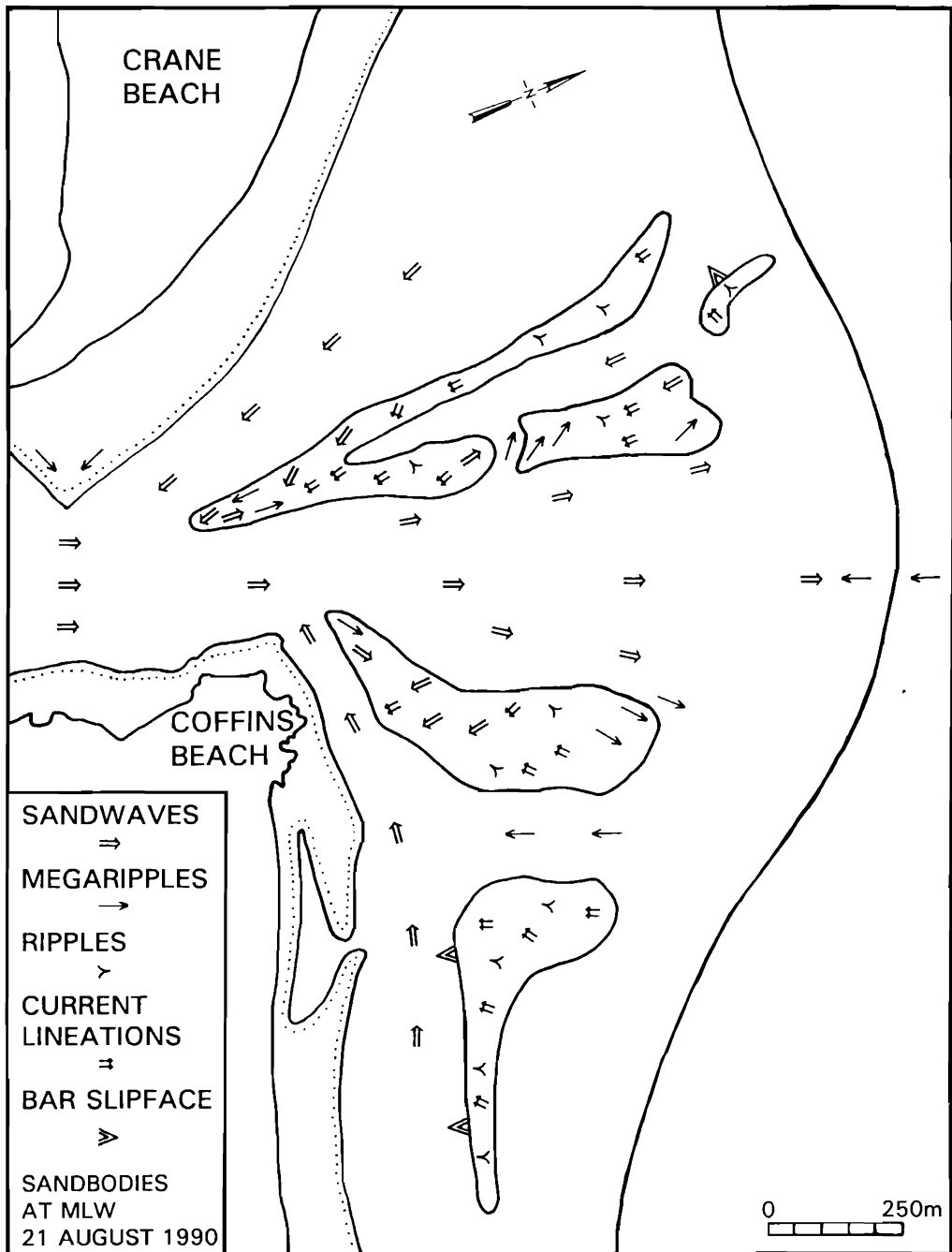


Figure 7. Bedform distributions recorded on the delta on 21 August 1990 at low tide. Note predominance of ebb-oriented bedforms in the main ebb channel, landward-oriented bedforms on the adjacent swash platform, and inlet-oriented bedforms in the main ebb channel.

tidal delta ($d_m = 1.83\phi$) and Coffins Beach ($d_m = 1.86\phi$). This pattern is in contrast to the overall decrease in grain size along the barrier chain from Plum Island to southern Coffins Beach (Figure 1) (SHALK, 1936; GOODBRED and MONTELLO, 1989). This pattern observed at the inlet may be explained by the introduction of coarse-grained sediments during periods of spring freshets from the Castle Neck and Essex Rivers.

An additional less apparent trend is that sediments of tide-dominated environments (main ebb channel and marginal flood channel) are composed of well- to very well-sorted medium sand ($d_m = 1.94\phi$) as compared to wave-dominated environments such as the swash bars and channel margin linear bars whose sediments consist of well-sorted fine sand ($d_m = 2.11\phi$). Sediments in the main ebb channel ($d_m = 1.85\phi$) are slightly coarser than those in the downdrift and updrift marginal flood channels ($d_m = 1.94\phi$ and 2.03ϕ , respectively).

Bedforms

The main ebb channel is floored by ebb-oriented bedforms throughout the tidal cycle, excepting the terminal lobe region where flood-oriented bedforms dominate. Generally, the bedforms decrease in both height and spacing in a seaward direction (Figure 3). At the inlet throat, sandwaves ($\lambda > 6.0$ m; BOOTHROYD and HUBBARD, 1974) are up to 40.0 m in spacing and 1.0 m in height (Figure 3, Profile C-D) but reduce to 15.0 m in spacing and 1.2 m in height just seaward of the inlet throat (Figure 3, Profile E-F). Approximately 1 km from the throat section, bedforms reduce to less than 7.0 m in spacing and 1.0 m in height (Figure 3, Profile E-F; Figure 2B, #1). At seaward, portions of the main ebb channel (in the vicinity of the terminal lobe), poorly-formed ebb-oriented megaripples ($0.6 \text{ m} < \lambda < 6.0 \text{ m}$; BOOTHROYD and HUBBARD, 1974), are up to 4.0 m in spacing and 0.6 m in height. These bedforms grade seaward to well-developed, flood-oriented megaripples associated with wave-generated landward-directed currents ($\lambda = 5.5$ m; $h = 0.7$ m) (Figure 3, Profile F-G).

Both the north and south marginal flood channels near the main ebb channel are dominated by flood-oriented bedforms. Sandwaves in the updrift marginal flood channel ($\lambda = 20.0$ m; $h = 1.5$ m) remain flood-oriented throughout the tidal cycle (Figure 5, Profile A-B; Figure 2B, #2). Sandwaves in the southern marginal flood channel (λ

Table 3. Changes in sediment volume for Crane and Coffins Beaches, and for intertidal offshore sand bodies during the 14-month period from Summer 1989 to Summer 1990. Note the overall inversely proportional relationship between offshore intertidal bar and beach sediment volume.

Location	Volume Changes
Updrift	
Updrift Channel Margin	
Linear Bar	Increase 5,900 m ³
Crane Beach (to 900 m north of Inlet)	Decrease 170,000 m ³
Downdrift	
Downdrift Channel Margin	
Linear Bar	No Change
Downdrift Swash Bar	Increase 51,000 m ³
Coffin Beach (to 900 m south of Inlet)	Decrease 40,000 m ³

$= 10.0$ m; $h = 1.0$ m) occasionally change orientation late in the ebb cycle (Figure 5, Profile C-D).

A bedform map of the ebb-tidal delta, including the trend of bar slipfaces, documents the general patterns of sediment transport in which landward transport on both sides of the delta platform is countered by seaward transport in the main ebb channel (Figure 7). Note also that sandwaves dominate the tidal channels while ripples ($\lambda < 0.6$ m; BOOTHROYD and HUBBARD, 1974), plane beds, and current lineations cover the wave-dominated delta platform. Seaward-oriented bedforms are limited to areas affected by ebb currents flowing out the main ebb channel including portions of the channel margin linear bars adjacent to the main ebb channel (Figure 2C).

Historical Morphologic Changes

Short-term Changes

Morphologic changes to the ebb-tidal delta during the study period (June 1989 to August 1990) included: 1) volumetric increase of the swash bars on the ebb-tidal delta; 2) a southerly migration of the seaward portion of the main ebb channel and; 3) onshore movement of bar complexes.

The enlargement of ebb-tidal delta bars included volumetric increases of the northern channel margin linear bar by 5,900 m³ and the southern swash bar complex by 51,000 m³ (Table 3). The volume of the downdrift channel margin linear bar remained unchanged during the study period. Coincident with the increase in the bar complexes was extensive erosion along both Crane and Coffins Beaches.

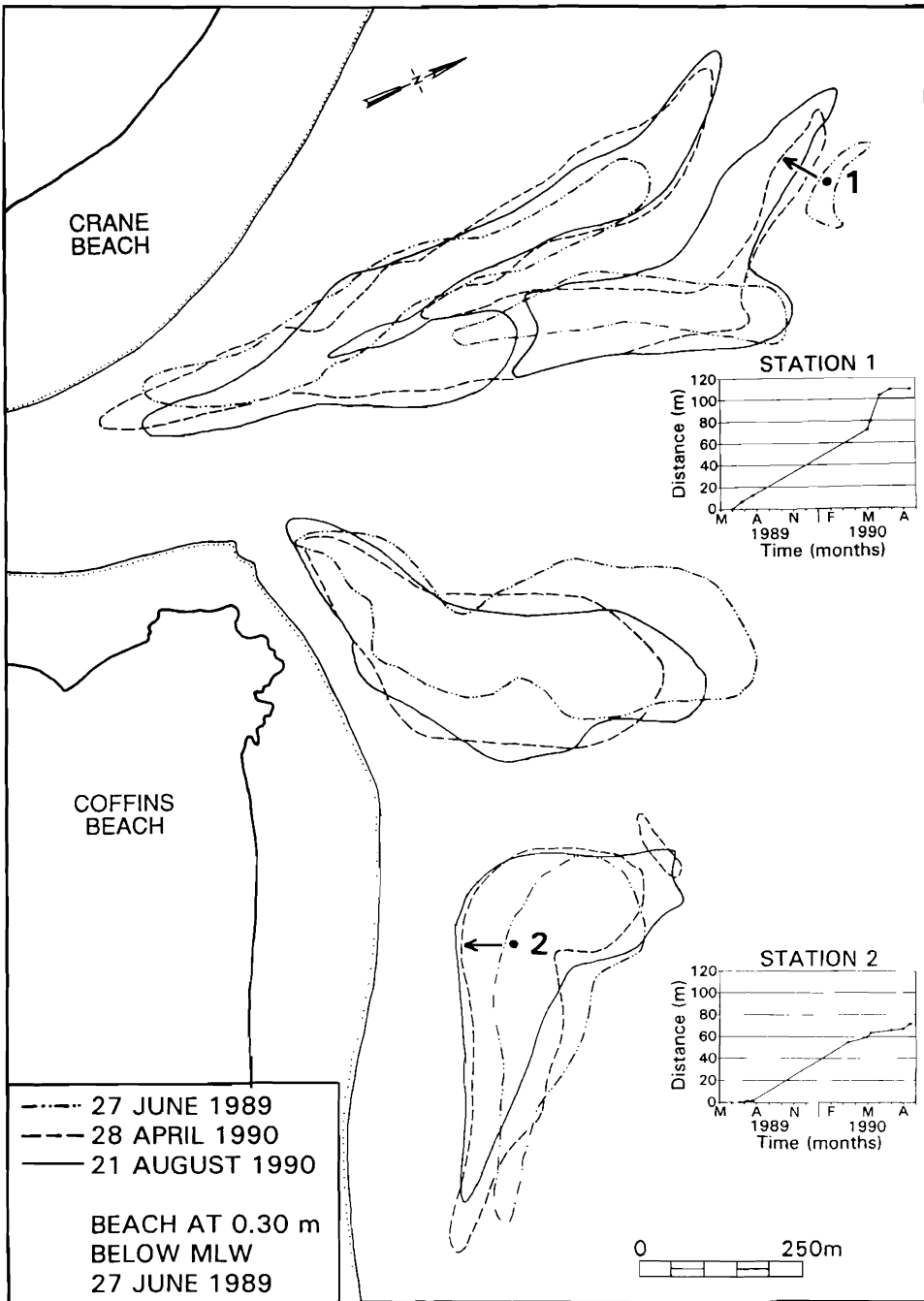


Figure 8. Comparison of intertidal sand bodies at 0.30 m below mean low water during a 14-month period from Summer 1989 to Summer 1990.

fins Beaches (170,000 m³ and 40,000 m³, respectively) (Figure 11; Table 3). This suggests that a relationship exists between changes in beach and offshore bar volume (*e.g.* FITZGERALD, 1984). It appears that erosion of the beach introduces large quantities of sand into the inlet throat, transporting it seaward to the ebb-tidal delta. This process results in an overall increase in the volume of the ebb-tidal delta during the study period.

The seaward portion of the main ebb channel migrated clockwise (southerly) by 100 m. This movement of the channel appears to be the result of bar formation on the updrift side of the main ebb channel. Presumably, the supply of sand for this construction came from the sediment transported out of the main ebb channel.

The onshore transport of sand on the ebb-tidal delta was evidenced by the landward migration of the updrift bar complexes (100 m) over the 14-month study period (Station 1 of Figure 8). The migration rate of individual swash bars on the distal portion of the delta averaged 0.20 m/day, however, during moderate NE storms (28 April 1990; 4 May 1990) the rate increased to greater than 1 m/day. The downdrift bar complexes (Station 2 of Figure 8; Figure 2D) migrated 75 m onshore during the 14-month study period.

Long-term Changes

Similar changes to the ebb-tidal delta have been documented in sequential vertical aerial photographs covering a 42-year period from 1943–1985 (Figure 9; Table 4). During this period, the ebb-tidal delta has undergone changes in size, extent of intertidal swash bars, position and orientation of the main ebb channel, and in the development of beach ridges along the adjacent beaches. The most important of these changes has been the formation, landward migration, and attachment of the swash bars to the onshore beach. For example, note in Figure 9 that several bar complexes migrated onshore, building beach ridges on both sides of the inlet shoreline between 1965 and 1977. Between 1943 to 1985, it also appeared that the main ebb channel migrated south coincident with the buildup of sediment on the updrift side of the delta.

DISCUSSION

Sediment Circulation Patterns

Wave and tidal processes at the Essex River Inlet produce sand circulation gyres between the

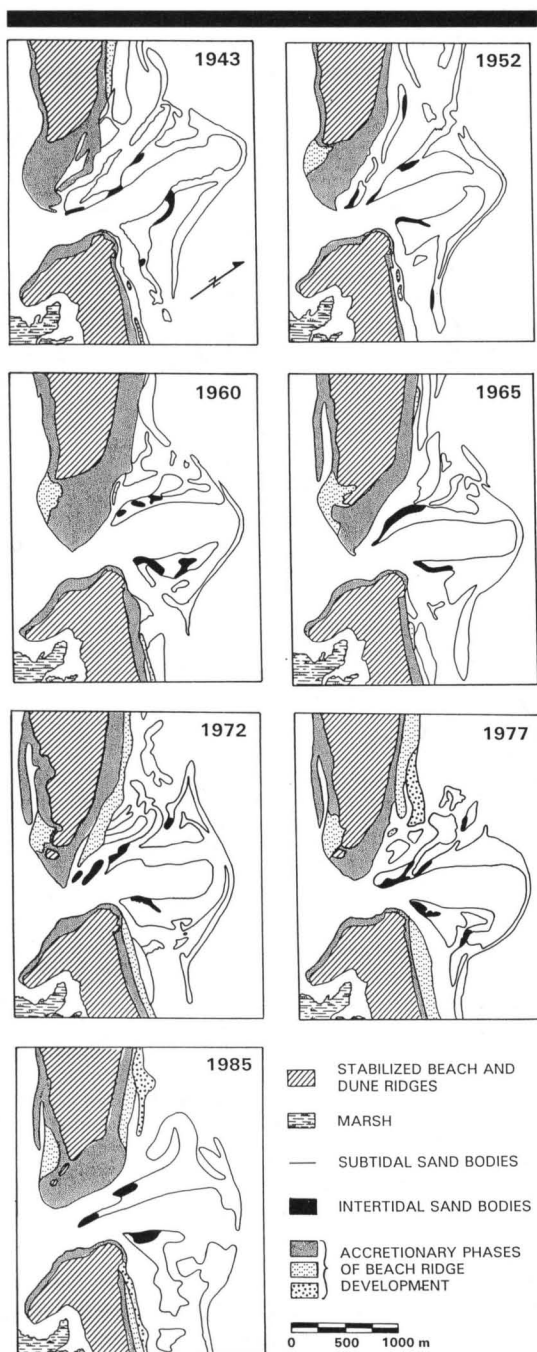


Figure 9. Morphologic changes of the Essex River ebb-tidal delta as determined from vertical aerial photograph overlays for the period 1943–1985. Note the clockwise (southerly) migration of the outer main ebb channel, stability of the inlet throat, and overall accretion through beach ridge development of both Crane and Coffins Beaches.

Table 4. *Historical morphological changes to the Essex River ebb-tidal delta and surrounding environments determined from historical aerial photographs.*

Date	Overall Interpretation	Main Ebb Channel Configuration	Marginal Flood Channel/ Swash Platform Channel Characteristics
07 July 1943	Small sediment volume of ETD. Majority of sediment is offshore but is migrating onshore. Well defined marginal flood channel (MFC).	Most seaward extent of MEC during period (1.47 km from Coffin Beach headland). Entire main ebb channel (MEC) has slight updrift-offset position.	Well-defined updrift and down-drift MFC. Swash platform channel (SPC) in between down-drift CMLB and down-drift swash bar is nonexistent.
26 July 1952	Great ETD volume as sand moves onshore and CMLB increase in size.	Less seaward extent of MEC (1.25 km). MEC has shore normal orientation and is wider at distal portions.	Well-defined updrift and down-drift MFCs. SPC is nonexistent.
19 May 1960	Swash bar migration has resulted in great sediment volume at proximal portions. Accretionary phases at both beaches. Distal MEC has down-drift-offset configuration.	Near similar seaward extent of MEC (1.22 km). Channel has shore normal orientation and has similar width to 1952. Outer MEC has slight down-drift-offset configuration.	MFCs are well defined. Swash platform channel is present and separates down-drift CMLB from down-drift swash bar.
04 April 1965	Great volumes of sediment at proximal portions of ETD and at CMLB. Both beaches have depleted greatly in sediment. Distal MEC has down-drift-offset configuration.	Near similar seaward extent of MEC (1.23 km). Distal MEC has more down-drift-offset configuration.	Well-defined updrift MFC but poorly defined down-drift MFC. Down-drift swash channel is non-existent; swash bar is migrating onshore in its place.
13 May 1972	Great sediment volume throughout system. Distinct phases of swash bar migration, particularly updrift. Outer MEC is at extreme down-drift-offset position. Well defined MFC's and swash platform channel.	Similar seaward extent of MEC with greater down-drift offset configuration. Outer MEC is at farthest down-drift-offset position of entire historical study.	Well-defined updrift and down-drift MFC's and down-drift swash platform channel.
01 April 1977	Great amounts of sediment in proximal portions but little sediment distally.	Similar seaward extent of MEC (1.23 km). MEC has widened since 1972 but still has slight down-drift-offset configuration.	Well-defined down-drift MFC. Poorly developed updrift MFC and swash platform channel.
29 Sept. 1985	Majority of ETD sediment is in distal locations. Beaches have small sediment volume. No distinct phase of swash bar migration.	Similar seaward extent of MEC. Distal MEC has slight down-drift-offset configuration.	Well-defined updrift and down-drift MFC's. Swash platform channel just present.

main ebb channel and the adjacent updrift and down-drift platform (Figure 10). Sediment is introduced to the main ebb channel through the marginal flood channel and across the channel margin linear bars. Sand in the main ebb channel is transported in a net seaward direction to the terminal lobe by the dominant ebb-tidal currents. Sandwave migration appears to be the primary mechanism in the process. Sand in the terminal

lobe region is moved back onshore by flood-tidal and wave-generated currents in the form of migrating swash bars. In the updrift portion of the delta, the counterclockwise gyre is completed as small swash bars ($\sim 8,000 \text{ m}^3$) attach to Crane Beach. In the down-drift portion of the delta, multiple swash bars migrate onshore forming a large bar complex ($\sim 135,000 \text{ m}^3$). The landward migration and attachment of the bar complex to

Table 4. *Extended.*

Swash Bar Position and Size	Channel Margin Linear Bar Morphology	Beach Morphology
Distinct phases of onshore migration of swash bars, both updrift and downdrift. Downdrift swash bar is connected to downdrift CMLB.	Updrift CMLB has large intertidal area and is aligned in an updrift position due to updrift-offset alignment of MEC. Downdrift CMLB has small size with intertidal portions at distal end.	Crane Beach is wide near inlet and spit but narrows to the northwest. Coffins Beach is narrow with slight bulge about 350 m to southeast of bedrock at Twopenny Loaf.
Downdrift swash bars well offshore of Coffins Beach.	Updrift CMLB has small intertidal portion but overall increase in size. Downdrift CMLB has more downdrift position with intertidal position closer to Coffins Beach adjacent to MFC.	Beach morphology similar to 1943. Swash bars near to and nearly accreted onto beaches.
No distinct phase of onshore swash bar migration.	Updrift and downdrift CMLB has remained constant in size with similar intertidal areas as 1952.	Width of Crane and Coffins Beaches has increased due to welding of swash bars previously. Second phase of beach ridge development present.
Distinct phase of onshore migration of swash bars for both updrift and downdrift portions. Positions of swash bars are relatively far offshore.	Both updrift and downdrift CMLB are large in size with majority of sediment at proximal locations. Downdrift CMLB connected to downdrift swash bar.	Coffins Beach, Crane Beach and spit system on southern end of Crane Beach substantially decrease in sediment.
Distinct phase of swash bar migration onshore. Note five phases of swash bar migration in updrift portions of ETD. Downdrift, one large swash bar lies well offshore.	Both updrift and downdrift CMLB are large in size with greatest intertidal portions landward near MFC's. Downdrift CMLB connected to downdrift swash bar.	Substantial welding of swash bars to both Crane and Coffins Beaches. Spit system still has small sediment volume.
Distinct phase of swash bar migration onshore for both updrift and downdrift portions. Great southeastern extent of downdrift swash bar.	Updrift CMLB is similar in size to 1972. Intertidal portions of CMLB are landward near MFC. Distally, downdrift CMLB is depleted of sediment but has great amount intertidal portions abutting MFC.	Swash bars welding to beach especially on Crane Beach. Spit system has increased in area substantially.
Less distinct phase of swash bar migration than in previous years. Swash bars are mostly offshore for both updrift and downdrift portions.	Updrift CMLB is slightly smaller than in 1979. Majority of CMLB sediment is in distal portions. Downdrift CMLB is very small but does connect to downdrift swash bar.	Narrowing of both Crane and Coffins Beaches.

Coffins Beach occurs approximately every 5 to 7 years. The clockwise sediment gyre is completed as sand is transported along Coffins Beach and into the inlet channel.

Growth and Decay of the Ebb-Tidal Delta

The field data and historical aerial photographs document the short and long term changes that occur to the Essex River Inlet ebb-tidal delta. On the basis of this information, a conceptual model

has been constructed showing volume fluctuations of the ebb-tidal delta in response to the formation, landward migration and attachment of bar complexes to the landward beach (*cf.* HINE, 1975; FITZGERALD, 1976; SHA, 1990). The enlargement and reduction of the ebb-tidal delta involve erosion and accretion along adjacent beaches as well as sediment contributions from and exports to the regional southerly transport system.

The cycle of change of the ebb-tidal delta has

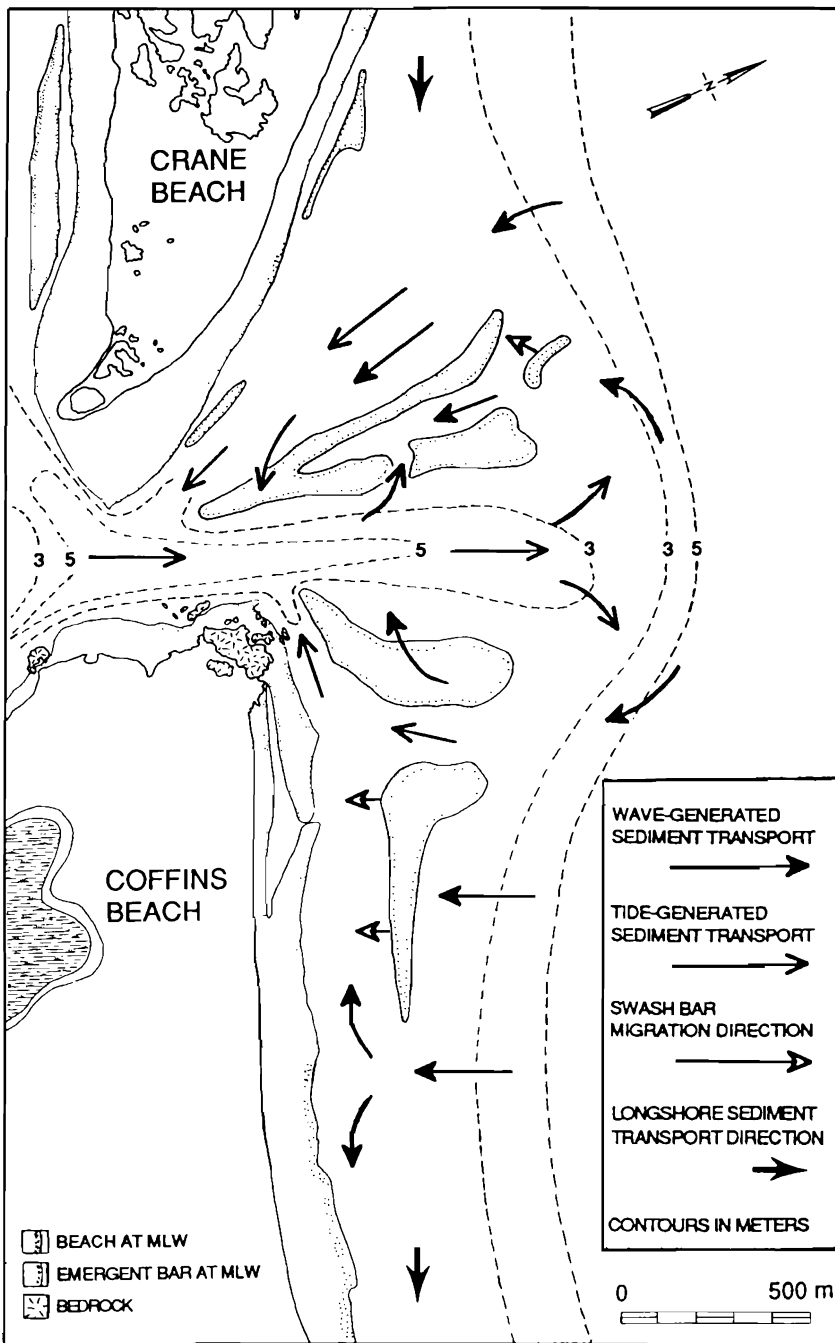


Figure 10. Sand circulation patterns at the Essex River ebb-tidal delta as determined from bar migrations, current measurements, bedform orientations, and historical morphological changes.

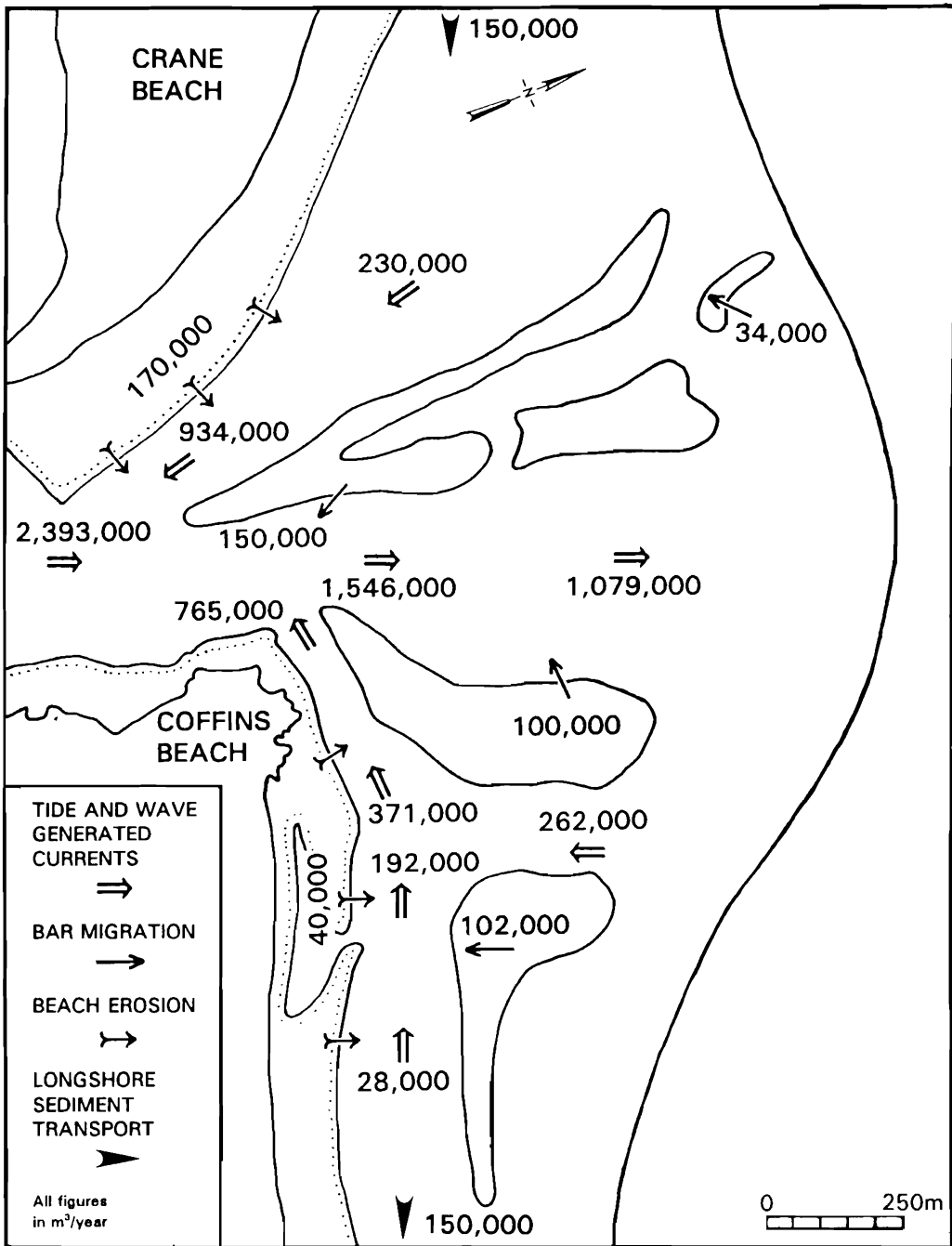


Figure 11. Potential transport rates of sand within channel systems on the ebb-tidal delta using MADDOCK's (1969) equation. Potential transport of sand on the swash bar was determined by swash bar migration rates. These are likely minimum estimates.

a periodicity of 5 to 7 years and can be divided into three stages. In Stage 1, the delta has a relatively small volume and there are few intertidal sand bodies, other than those associated with the channel margin linear bars, which persist through all stages (1943, 1965, 1985 depiction of delta; Figure 9). Due to the overall low elevation of the swash platform during this condition, the landward beaches are susceptible to storm erosion which contributes sand to the main ebb channel and ultimately to the ebb-tidal delta.

During Stage 2, swash bars form along the terminal lobe portion of the ebb-tidal delta, migrate onshore, and often attach to the channel margin linear bars, forming large bar complexes (1952, 1977 depictions of ebb-tidal delta; Figure 9). The growth of these bar complexes changes the distribution of wave energy over the delta, resulting in lower wave energy along the landward beaches. During dominant northeast wave conditions, the refraction of waves around the southern bar complex produces a longshore transport reversal along Coffins Beach. The littoral transport reversal is maintained as long as the bar complex is at least 100 to 200 m offshore. During this period, sediment is trapped within the inlet complex and there is continual growth of the ebb-tidal delta. At the end of Stage 2, as the bar complexes migrate close to the beach (< 100 m), the marginal flood channels are gradually constricted resulting in stronger tidal- and wave-generated currents which commonly produce beach erosion.

During the final stage of the cycle (1960, 1972 depictions of the ebb-tidal delta; Figure 9), bar complexes on the ebb-tidal delta weld to the adjacent shoreline, delivering 100,000 m³ to 200,000 m³ of sand to the beach. After the welding event, the beach is significantly widened but this condition is temporary. At the end of Stage 3, the lack of bar complexes on the ebb-tidal delta results in greater wave energy along the inlet beaches. During this period the inlet shoreline erodes; sand is transported to the inlet throat and, in the case of the downdrift inlet shoreline, released to Coffins Beach.

The model described above is similar to one envisioned for Price Inlet, South Carolina (FITZGERALD, 1984) with the exception that the channel margin linear bars at the Essex River ebb-tidal delta are well established and do not change significantly during the different morphological stages. Volumetric changes to ebb-tidal deltas have been documented at other tidal inlets along the

South Carolina coast (FINLEY, 1978; FITZGERALD, 1984), New Jersey Coast (Barnegat Inlet; ASHLEY *et al.*, 1981), the Netherland Coast (SHA, 1990), and Florida (East Pass; MORANG, 1992). At most of these locations, bar complexes form on the swash platform of the ebb-tidal delta, migrate onshore, and attach to the landward beach. Thus, it would appear that the conceptual models described for Price Inlet, South Carolina (FITZGERALD, 1984) and the Essex River may have a wider application.

Potential Sediment Transport Rates

A variety of means were employed to determine patterns and relative rates of sand transport throughout the delta. Transport rates in channels were approximated utilizing a form of MADDOCK'S (1969) equation that has been used at other tidal inlets (FITZGERALD *et al.*, 1976; HUBBARD *et al.*, 1977). This equation is based on current velocities in which the *maximum potential load* is proportional to the cube of the velocity:

$$\text{Load (in m}^3\text{/sec)} = 15.244 V^3/1,600$$

where V is the maximum velocity (m/sec). For this analysis, velocities were integrated over a complete tidal cycle for mean tidal conditions using one to four stations across the channels. Although developed for fluvial systems, MADDOCK'S (1969) equation is useful for determining qualitative estimates of sand transport in tidal inlet channels particularly for comparing transport rates within an ebb-tidal delta system. The sediment transport rates determined in this analysis do not consider the reduction in current velocity along the sides of the channel, and therefore are probably maximum values. It should be noted that other equations exist that may more accurately model sediment transport conditions in tidal channels (*i.e.* MADSEN and GRANT, 1976; ENGELUND and HANSEN, 1967). However, they require more detailed hydraulic data than were collected in this study.

Sediment transport rates across the swash platform were estimated from the migrations of bar complexes. Migration rates were determined by multiplying the distance the slipface had migrated by the bar length and thickness and subsequently divided by the period of record. These calculations indicate that a minimum of 3.4×10^4 m³ of sand is transported to the updrift beach each year, and that a minimum of 1.0×10^5 m³ of sand is delivered to the downdrift beach (Figure 11).

Sediment transport calculations for the inlet throat during mean tidal conditions show a potential net ebb sediment transport rate of $2.39 \times 10^6 \text{ m}^3/\text{year}$ (Figure 11), or 68% of the total ebb-tidal delta volume of $3.53 \times 10^6 \text{ m}^3$. The actual volume of sand transported in this region of the inlet is probably less due to a shell lag that floors this portion of the channel bottom. Sand transport in the main ebb channel decreases in a seaward direction to $1.50 \times 10^6 \text{ m}^3/\text{year}$ halfway out the main ebb channel (Station 5, Figure 4) and to $1.10 \times 10^6 \text{ m}^3/\text{year}$ in the vicinity of the terminal lobe (Station 6, Figure 4). These values compare with a calculated rate of $1.70 \times 10^6 \text{ m}^3/\text{year}$ of sediment introduced into the main ebb channel from the marginal flood channels (9.34×10^5 and $7.65 \times 10^5 \text{ m}^3/\text{year}$ from the updrift and downdrift marginal flood channels, respectively), and $2.50 \times 10^6 \text{ m}^3/\text{year}$ of sediment transported across the channel margin linear bars. This quantity of sand can be easily removed from the main ebb channel by the ebb currents. The decrease in the sand transport out the main ebb channel results in sand deposition in the distal portion of the channel margin linear bars, where it is reworked back onshore by wave action and flood-tidal currents.

It is evident that if MADDOCK's (1969) equation gives true estimates of the volume of sand moved through the inlet channels (Figure 11), then far more sand is circulated within the delta system than is involved in bypassing sand around the inlet (approximated by the longshore transport rate, $1.50 \times 10^6 \text{ m}^3/\text{year}$). Moreover, if the long-term offshore versus onshore sand transport rates are equal at the inlet, which must be true if historically the delta remains the same size, then the landward movement of sand across the swash platform must be an order-of-magnitude greater than that contained in the landward migrating bar complexes. Supporting this conclusion is the likelihood that sand moved across the swash platform is only partially captured on the bar slipfaces. Fieldwork at Murrells Inlet, South Carolina demonstrated that the suspended load (wave-suspended sand) moved across a swash bar can be an order-of-magnitude greater than the bedload shown by migration of the bar slipface (HUBBARD *et al.*, 1977). Thus, it appears that the sediment gyres at the Essex River Inlet ebb-tidal delta circulate much greater quantities of sand than the amount indicated by the morphologic changes at the inlet.

Comparison With Other Ebb-Tidal Deltas

The Essex River Inlet ebb-tidal delta is similar to those of other mixed-energy, tide-dominated inlets, having well-developed marginal flood channels and main ebb channel, swash platform, intertidal channel margin linear bars and swash bars. Morphologically, Essex River Inlet is most like the Central South Carolina inlets (*e.g.* in size of the ebb-tidal delta and intertidal exposure of sand bodies). Their comparable size is due to similar tidal prisms, whereas their similar extent of intertidal bars is probably a function of tidal range and offshore slope. The steeper offshore slope in Northern Massachusetts as compared to Central South Carolina is compensated by its greater tidal range which leads to equivalent exposure of sand bodies at low tide. With respect to tidal energy, Northern Massachusetts inlets experience a mean and spring tidal range approaching that of the Gulf of Alaska Copper River Delta inlets. However, the Gulf of Alaska inlets have much larger backbarrier areas which result in order-of-magnitude larger tidal prisms and throat cross-sectional areas. Despite these differences, the offshore extent of the ebb-tidal delta at both inlet locations is approximately the same (Northern Massachusetts = 2,000 m, Copper River Delta = 2,300 m; Table 1). The diminutive size of the Copper River Delta ebb-tidal deltas is probably related to the relatively large wave energy of the Gulf of Alaska (deepwater wave heights of 1.50 m) and wide inlet channels. These conditions would be expected to cause a relatively rapid decrease in strength of the ebb jet away from the inlet throat such that sediment is not transported very far offshore.

Inlets along the Netherland and German Friesian Island Coasts are much larger than Northern Massachusetts inlets; they are characterized by lower tidal ranges, particularly along the West Friesian Islands and greater wave energy, especially in the East Friesian Islands, and larger backbarrier areas. The ebb-tidal deltas of the North Sea are many times larger than that of the Essex River Inlet due to order-of-magnitude larger tidal prisms. In spite of this difference in scale, the sand circulation processes appear to be similar at both locations with sand bypassing occurring, in part, by the landward migration and attachment of bar complexes from the delta to the downdrift barrier (HOMEIER and LUCK, 1969; NUMMEDAL and PENLAND, 1981; SHA, 1989).

The southern New Jersey and Virginia Inlets are slightly larger than the Northern Massachusetts inlets, and sand bodies are less well formed. This may reflect the smaller wave energy and tidal range of the mid-Atlantic coast. Lower wave energy results in poorer swash bar development, and lower tidal range provides less intertidal exposure of sand bars on the swash platform. A similar case can be made for the poorer development of intertidal sand bodies at Georgia ebb-tidal deltas.

CONCLUSIONS

(1) Essex River Inlet is an ebb-dominated system. This ebb dominance, which exists during periods of greater than average tidal ranges and especially during spring tides, is evidenced by ebb-oriented bedforms at the inlet throat and along the inlet channel. The marginal flood channels, floored by flood-oriented bedforms, are the primary conduit of sand being transported into the main ebb channel.

(2) The movement of sand within the ebb-tidal delta is characterized by two sediment circulation gyres involving the main ebb channel and adjacent swash platforms. One element of these sand gyres is the formation, landward migration, and attachment of bar complexes to the inlet beaches. Sediment transport rates calculated for the inlet channels using MADDOCK's (1969) equation indicate that a much larger quantity of sand is moved in the marginal flood channels and main ebb channel than is delivered to the inlet through long-shore sediment transport and eventually bypasses the inlet. These estimates infer that the volume of sand moved landward over the swash platform, as part of the sediment gyres, is an order-of-magnitude greater than the volume of sand moved onshore via storage in the bar complexes. The volume of sand circulated within the sediment gyres is estimated to be more than a million cubic meters per year.

(3) The major morphologic changes to the ebb-tidal delta during the 14-month study period included an overall increase in its volume, a southerly migration of the seaward portion of the main ebb channel of 100 m, and the onshore movement of southern bar complex of 80 m. Historical data suggest that these changes are part of a 5- to 7-year ebb-tidal delta cycle of growth and decay. The volume of the delta increases when bar complexes become well-developed and the refraction of waves around them leads to sand trapping within the delta complex. The delta decreases in vol-

ume when the bar complexes migrate onshore and weld to the beach.

(4) In comparison to other mixed-energy tide-dominated inlets, the Essex River ebb-tidal delta is most like the ebb-tidal deltas of Central South Carolina inlets both in its size and the exposure of intertidal sand bodies. The same approximate volume of the deltas is due to similar tidal prisms. The pattern of sand circulation documented at the Essex River Inlet ebb-tidal delta is similar to that of ebb-tidal deltas along the Netherland and German Friesian Islands, Central South Carolina, and other mixed-energy, tide-dominated inlets.

ACKNOWLEDGEMENTS

Appreciation is expressed to numerous people for their assistance during the field investigation phase of the project. The authors acknowledge Sytze von Heteren and Terri Prickett for their review of the document. Assistance in generating figures was provided by Andrew Morang. The Chief of Engineers of the United State Army Corps of Engineers is acknowledged for granting permission to publish the paper.

LITERATURE CITED

- ANAN, F.S., 1971. Provenance and statistical parameters of sediments of the Merrimack Embayment, Gulf of Maine. Ph.D. Thesis, Amherst, Massachusetts: University of Massachusetts, Department of Geology and Geography, 185p.
- ASHLEY, G.M.; HALSEY, S.D., and FARRELL, S.C., 1981. Growth and modification of an ebb-tidal delta sand body in response to changes in sediment supply and hydrographic regime. *Geological Society of America: Northeastern Section, Abstracts with Programs*, 13, 121.
- AUBREY, D.G. and SPEER, T.E., 1985. A study of non-linear tidal propagation in shallow inlet/estuarine systems, Part I: Observations. *Estuarine and Coastal Shelf Science*, 21, 185-205.
- BOON, J.D. and BYRNE, R.J., 1981. On basin hypsometry and morphodynamic response of coastal inlet systems. *Marine Geology*, 40, 27-48.
- BOOTHROYD, J.C. and HUBBARD, D.K., 1974. *Bedform Development and Distribution Pattern, Parker and Essex Estuaries, Massachusetts*. Miscellaneous Paper CERC-1-74, U.S. Army Engineers Waterways Experiment Station, Vicksburg, Mississippi, 39p.
- BOYD, R.; BOWEN, A.J., and HALL, R.K., 1987. An evolutionary model for transgressive sedimentation on the eastern shore of Nova Scotia. In: FITZGERALD, D.M. and ROSEN, P. (eds.), *Glaciated Coasts*. New York: Academic, pp. 87-114.
- DEAN, R.G. and WALTON, T.L., 1975. Sediment transport processes in the vicinity of inlets with special reference to sand trapping. In: CRONIN, L.E. (ed.), *Estuarine Research, Vol. 2: Geology and Engineering*. New York: Academic, pp. 129-149.

- EDWARDS, G., 1988. The Late Quaternary Geology of Northeastern Massachusetts in the Merrimack Embayment, Western Gulf of Maine, M.A. Thesis, Boston, Massachusetts: Boston University, 185p.
- ENGELUND, F. and HANSEN, E., 1967. A monograph on sediment transport in alluvial streams. *Teknisk Vortlag*, Copenhagen, Denmark.
- FINLEY, R.J., 1978. Ebb-tidal delta morphology and sediment supply in relation to seasonal wave energy flux, North Inlet, South Carolina. *Journal of Sedimentary Petrology*, 48, 227-238.
- FITZGERALD, D.M., 1976. Ebb-tidal delta of Price Inlet, South Carolina: Geomorphology, physical processes and associated changes in inlet shape. In: HAYES, M.O. and KANA, T.W. (eds.), *Terrigenous Clastic Depositional Environments*. Report 11-CRD, Department of Geology, Univ. of South Carolina, Columbia, South Carolina, pp. II-143-II-157.
- FITZGERALD, D.M., 1984. Interactions between the ebb-tidal delta and landward shoreline: Price Inlet, South Carolina. *Journal of Sedimentary Petrology*, 54(4), 1303-1318.
- FITZGERALD, D.M., 1993. Origin and stability of tidal inlets in Massachusetts. In: AUBREY, D. and GIESE, G. (eds.), *Formation and Evolution of Multiple Tidal Inlets*, American Geophysical Union Special Publication, pp. 1-61.
- FITZGERALD, D.M. and FITZGERALD, S.A., 1977. Factors influencing tidal inlet throat geometry. *Coastal Sediments '77*, 563-581.
- FITZGERALD, D.M. and NUMMEDAL, D., 1983. Response characteristics of an ebb-dominated inlet channel. *Journal of Sedimentary Petrology*, 53, 833-845.
- FITZGERALD, D.M.; NUMMEDAL, D., and KANA, T.W., 1976. Sand circulation patterns at Price Inlet, South Carolina. *Proceedings of the 15th Coastal Engineering Conference*, 1868-1880.
- FITZGERALD, D.M.; PENLAND, S., and NUMMEDAL, D., 1984. Changes in tidal inlet geometry due to back-barrier filling: East Friesian Islands, West Germany. *Shore and Beach*, 52, 3-9.
- GOODBRED, S.L. and MONTELLIO, T.M., 1989. *A Study of the Morphological Characteristics of Plum Island, Crane, Coffins, and Wingsheek Beaches, Massachusetts*. Geology Department, Boston University, 15 p.
- HAYES, M.O., 1975. Morphology of sand accumulation in estuaries: An introduction to the symposium. In: CRONIN, L.E. (ed.), *Estuarine Research, Vol. 2: Geology and Engineering*. New York: Academic, pp. 3-22.
- HAYES, M.O., 1976. Geomorphology of the Southern Coast of Alaska. *Proceedings 15th Coastal Engineering Conference*, pp. 1992-2008.
- HAYES, M.O., 1977. Part 1—Lecture Notes. In: HAYES, M.O. and KANA, T.W. (eds.), *Terrigenous clastic depositional environments*. *Technical Report 11-CRD*, Department of Geology, University of South Carolina, Columbia, South Carolina, pp. I-1-I-74.
- HAYES, M.O., 1979. Barrier island morphology as a function of tidal and wave regime. In: LEATHERMAN, S.P. (ed.), *Barrier Islands: From the Gulf of St. Lawrence to the Gulf of Mexico*. New York: Academic, pp. 1-28.
- HINE, A.C., 1975. Bedform distribution and migration patterns on tidal deltas in the Chatham Harbor Estuary, Cape Cod, Massachusetts. In: CRONIN, L.E. (ed.), *Estuarine Research, Vol. 2: Geology and Engineering*. New York: Academic, pp. 235-252.
- HINE, A.C.; SNYDER, S.W., and NEUMANN, A.C., 1979. *Coastal Plain and Inner Shelf Structure, Stratigraphy and Geologic History: Bogue Banks Area, North Carolina: Part 3—The Holocene High Sedimentation Interval—An Hypothesis*. A Final Report to the North Carolina Science and Technology Committee, pp. 1-18.
- HOMEIER, H. and LUCK, G., 1969. Das Historische Kartenwerk 1:50,000 der Niedersächsischen Wasserwirtschaftsverwaltung, Cöttingen.
- HUBBARD, D.K., 1975. Morphology and hydrodynamics of the Merrimack River ebb-tidal delta. In: CRONIN, L.E. (ed.), *Estuarine Research, Vol. 2: Geology and Engineering*. New York: Academic, pp. 253-266.
- HUBBARD, D.K., 1977. Variations in Tidal Inlet Processes and Morphology in the Georgia Embayment. *Technical Report 14-CRD*, Department of Geology, University of South Carolina, Columbia, South Carolina, 79p.
- HUBBARD, D.K.; BARWIS, J.H., and NUMMEDAL, D., 1977. Sediment transport in four South Carolina Inlets. *Coastal Sediments '77*, 582-601.
- JARRETT, J.T., 1976. Tidal Prism-Inlet Area Relationships. *GITI Report 3*, U.S. Army Engineer Waterways Experimental Station, Vicksburg, Mississippi, 55p.
- JENSEN, R.E., 1983. Atlantic Hindcast, Shallow Water, Significant Wave Information. *WIS Report 9*, U.S. Army Engineer Waterways Experiment Station, Vicksburg, Mississippi.
- KEULEGAN, G.H., 1967. Tidal Flows in Entrances: Water Level Fluctuations of Basins in Communication with Seas. *Technical Bulletin 14*, Committee on Tidal Hydraulics, U.S. Army Engineer Waterways Experiment Station, Vicksburg, Mississippi.
- MADDOCK, T., JR., 1969. The Behavior of Straight Open Channels with Moveable Beds. *United States Geological Survey Professional Paper 622-A*, Washington, D.C., 70p.
- MADSEN, O.S. and GRANT, W.G., 1976. Sediment Transport in the Coastal Environment. *Report No. 209*. Department of Civil Engineering, Massachusetts Institute of Technology, Cambridge, Massachusetts.
- MCCORMICK, C.L., 1968. Holocene Stratigraphy of the Marshes at Plum Island, Massachusetts. Ph.D. Thesis, Boston, Massachusetts: University of Massachusetts.
- MCINTYRE, W.G. and MORGAN, J.P., 1964. Recent Geomorphic History of Plum Island and Adjacent Coasts. *Coastal Study Series*, Baton Rouge, Louisiana: Louisiana State University.
- MORANG, A., 1992. A Study of Geologic and Hydraulic Processes at East Pass, Destin, Florida. *Technical Report CERC-92-5*, U.S. Army Engineer Waterways Experiment Station, Vicksburg, Mississippi.
- MOTA-OLIVEIRA, I.B., 1970. Natural flushing ability in tidal inlets. *Proceedings of the 12th Coastal Engineering Conference*, pp. 1827-1844.
- NELLIGAN, D., 1982. Ebb-Tidal Delta Stratigraphy. M.A. Thesis, Columbia, South Carolina: University of South Carolina, 178p.
- NEWMAN, W.S.; MARCUS, L.F.; PARDI, R.P.; PACCIONE,

- J.A., and TOMECEK, S.M., 1980. Eustasy and deformation of the geoid: 1,000–6,000 radiocarbon years BP. In: MORNER, N.A. (ed.), *Earth Rheology, Isostasy, and Eustasy*. Chichester, England: John Wiley, pp. 555–567.
- NUMMEDAL, D.; OERTEL, G.F.; HUBBARD, D.K., and HINE, A.C., 1977. Tidal inlet variability—Cape Hatteras to Cape Canaveral. *Coastal Sediments '77*, 543–560.
- NUMMEDAL, D. and FISCHER, I., 1978. Process-response models for depositional shorelines: The German and Georgia Bights. *Proceedings of the 16th Coastal Engineering Conference*, pp. 1215–1231.
- NUMMEDAL, D. and HUMPHRIES, S.M., 1978. Hydraulics and Dynamics of North Inlet, South Carolina, 1975–1976. *GITI Report 16*, U.S. Army Engineer Waterways Experiment Station, Vicksburg, Mississippi.
- NUMMEDAL, D. and PENLAND, S., 1981. Sediment dispersal in Norderneyer Seegat, West Germany. *Special Publication of the International Association of Sedimentology No. 5*, pp. 187–210.
- OERTEL, G.F., 1975. Ebb-tidal deltas in Georgia estuaries. In: CRONIN, L.E. (ed.), *Estuarine Research, Vol. 2: Geology and Engineering*. New York: Academic, pp. 267–276.
- OLDALE, R.N., 1985. Late Quaternary sea-level history of New England: A review of the published sea-level data. *Northeastern Geology*, 7(3/4), 192–200.
- POSTMA, H. (ed.), 1982. *Hydrography of the Wadden Sea: Final Report on Hydrography of the Wadden Sea Working Group*. Sticht, Leiden: Veth Steun Waddenonderz, 77p.
- SHA, L.P., 1989. Sand transport patterns in the ebb-tidal delta off Texel Inlet, Wadden Sea, The Netherlands. *Marine Geology*, 86, 137–154.
- SHA, L.P., 1990. Surface sediments and sequence models in the ebb-tidal delta of Texel Inlet, Wadden Sea, The Netherlands. In: SHA, L.P. (ed.), *Sedimentological Studies of the Ebb-Tidal Deltas Along the West Friesian Islands, The Netherlands. Geological Ultraiectina No. 64*.
- SHALK, M.A., 1936. A Textural Study of Certain New England Beaches. Ph.D. Thesis, Cambridge, Massachusetts: Harvard University.
- SMITH, J.B., 1991. Morphodynamics and Stratigraphy of Essex River Ebb-Tidal Delta: Massachusetts, *Miscellaneous Report CERC-91-11*, U.S. Army Engineer Waterways Experiment Station, Vicksburg, Mississippi.
- SOM, M.R., 1990. Stratigraphy and the Evolution of a Backbarrier Region Along a Glaciated Coast of New England: Castle Neck-Essex Bay, Massachusetts. M.A. Thesis, Boston, Massachusetts: Boston University. 185p.
- U.S. ARMY CORPS OF ENGINEERS, 1984. *Shore Protection Manual*. U.S. Army Engineer Waterways Experiment Station, Vicksburg, Mississippi.
- U.S. DEPARTMENT OF COMMERCE, 1994. *Tide Tables, East Coast of North and South America*. National Oceanic and Atmospheric Administration, Rockville, Maryland, 301p.
- WALTON, T.L. and ADAMS, W.D., 1976. Capacity of inlet outer bars to store sand. *Proceedings of the 15th Coastal Engineering Conference*, pp. 1919–1937.